Talanta 104 (2013) 212–218

Contents lists available at SciVerse ScienceDirect

Talanta

journal homepage: www.elsevier.com/locate/talanta

Non-enzymatic electrochemical glucose sensor based on silver/silver oxide nano-rods reinforced with multiwall carbon nanotubes

Leila Shahriary, Santosh K. Haram, Anjali A. Athawale *

Department of Chemistry, University of Pune, Ganeshkhind, Pune 411 007, India

ARTICLE INFO

Article history:
Received 25 September 2012
Received in revised form
7 November 2012
Accepted 8 November 2012

Keywords:
Electrochemical
Non-enzymatic
Glucose
Sensor
MWCNTs
Silver

ABSTRACT

Silver/silver oxide nanorods reinforced with Multi[illegible]l ca[illegible]nanotub[illegible] (Ag/Ag_2O-f-MWCNTs), were prepared by electrophoretic dissolution of silve[illegible]ode in aq[illegible]us [illegible]ersion of HOOC-functionalized MWCNTs and tested for the amperometric s[illegible] of glucose. [illegible]ciation of native silver oxide and silver with f-MWCNTs was confirmed by R[illegible]an sp[illegible]roscopy, XRD and EDAX analysis in conjunction with cyclic voltammetry (CV). The electrocatalytic oxi[illegible]on of glucose at Ag/Ag_2O-f-MWCNT modified electrode in alkaline solution has bee[illegible]tigated in de[illegible]A plausible mechanism has been proposed for oxidation of glucose on Ag/Ag_2O[illegible]-MWCNTs based on cyclic voltammetric measurements. Current–time dynamic response at +0.60 V[illegible]ep potenti[illegible]s. Hg/HgO in NaOH (0.1 M) were recorded and linear response was obtained (R^2=0.978[illegible] a functi[illegible] of glucose concentration (0.5 mM–12 mM), with a detection limit of 5.5 μM (S/N ratio i[illegible]nd s[illegible]itivity of 17.2 $\mu A mM^{-1} cm^{-2}$. The signal corresponding to glucose was seen[illegible]unaffected[illegible]to interference from ascorbic acid, uric acid and chloride ions present in the sol[illegible]n. [illegible]NTs provide large surface area for electrochemical reaction and mechanical support to t[illegible] silv[illegible], which seems to be very important when Ag is repeatedly undergoing ph[illegible] transfor[illegible]n from $Ag \leftrightarrow Ag_2O \leftrightarrow AgO$ during glucose oxidation. An association of stable Ag_2O[illegible]as[illegible]ith silv[illegible] surface is a key feature of Ag/Ag_2O-f-MWCNTs in the glucose sensing applicati[illegible]

© 2012 Elsevier B.V. All rights reserved.

1. Introduction

Diabetes mellitus is a chr[illegible]c syn[illegible]me which is seldom cured, except in a very specifi[illegible]u[illegible]on. As[illegible]er World Health Organization (WHO) repor[illegible]ca. 3[illegible]billion[illegible]eople are expected to be affected by diabe[illegible] B[illegible]030 [illegible] monitoring of blood glucose is one of th[illegible]est wa[illegible] to cont[illegible] diabetes [2]. Amperometric biosensors [illegible]ol[illegible]h glucose oxidase (GO_x) have been studied ext[illegible]ely and are available commercially. Though, GO_x based biosen[illegible] are very selective and specific for the glucose [3], their acti[illegible]y and stability are affected by temperature, pH, humidity and interfering ions/biomolecules present in the blood serum [4]. Therefore, development of non-enzymatic glucose sensors (NEGS) has been the focus of intense research in the recent years. Metals such as gold [5], platinum [6], copper [7], their alloys [8], and metal oxides such as MnO_2 and CuO [9,10] have been examined extensively as electrode materials during early stages of development of NEGS. However, these electrodes have drawbacks such as poor selectivity and low sensitivity caused by surface poisoning due to absorbed chloride ions [8] and intermediates [11] formed during the glucose oxidation. Therefore, there is a great demand to develop enzyme free glucose sensors having an optimum sensitivity without compromising the stability. Recently, electrodes modified with nanoparticles (NPs) of metals [12–18] and metal oxides [19,20] have been examined for this purpose. Though, a large surface area to volume ratio and high mass transport associated with NPs enhances the sensitivity, catalytic activity and electrocatalytic activity compared to their bulk counterpart [21,22], the capping agents used to stabilize them may interfere and mask the desired properties. These limitations have been overcome by stabilizing them directly on non-metallic yet conducting support such as carbon nanotubes (CNTs) since, carbon nanotubes possess high chemical stability, mechanical strength, and electrical conductivity and also is resistant to poisoning by chloride ions [23]. Recently, functionalized carbon nanotubes decorated with NPs of Au, Pt/Cu_2S/SnO_2, CuO, Pd, Pt and Ni have been studied for enzyme free glucose sensors [24–29]. Unlike metal oxide supports, CNTs are known to be stable in biological environments. Besides, molecular interaction of CNTs with NPs is expected to play a synergistic role in overall electrochemical performance of the composite. However, improper coating of NPs may lead to partial exposure of CNTs which may impart large

* Corresponding author. Tel.: +91 25601395 566; fax: +91 2025691728.
E-mail address: agbed@chem.unipune.ac.in (A.A. Athawale).

0039-9140/$ - see front matter © 2012 Elsevier B.V. All rights reserved.
http://dx.doi.org/10.1016/j.talanta.2012.11.019

charging current compared to faradaic component, thereby affecting the sensitivity. This limitation can be overcome by ensuring proper coating of CNTs together with the synergistic effect of CNTs on metal. Besides, CNTs are expected to provide large surface area for uniform deposition of metal nanoparticles, a mechanical support to the metal along with an increase in its stability without compromising the sensitivity. To our knowledge, this approach has not yet been investigated so far in the sensor applications.

With this inspiration, in the present work, novel composite material consisting of silver nanorods, reinforced with MWCNTs (Ag/Ag_2O-f-MWCNTs) have been synthesized, characterized and suggested for its applicability as a non-enzymatic glucose sensor for the first time. The results reveal its potential applicability as a glucose sensor with negligible interference of uric acid (UA), ascorbic acid (AA) and chloride ions. Electrochemical sensing of glucose with composite electrode is driven by reaction of glucose with native silver oxides present on the surface of Ag/Ag_2O-f-MWCNTs. Interaction of MWCNTs with silver demonstrate synergistic role in electrochemical redox behavior of silver in alkali solution which is found to be advantageous in glucose oxidation. Choice of silver is due to formation of both, Ag_2O and AgO at sufficiently positive potentials [30,31]. AgO so formed at +0.75 V being unstable facilitates oxidation of glucose. Moreover, kinetics of formation of silver oxides is known to be very facile [32] which is advantageous in minimizing the response time. Furthermore, Ag_2O is reported to have high electrical conductivity (ca. 20 S cm^{-1}), which minimizes the current losses. MWCNTs function as a mechanical support to the silver films which is found to be very important when it is repeatedly phase transformed between silver and silver oxides phases, during glucose oxidation reaction.

2. Materials and methods

2.1. Chemicals and Materials

Ferrocene, naphthalene and benz[illegible]re purcha[illegible] from Fluka, S. D. Fine Chemicals and Merck, respe[illegible]ely. NaOH, NaCl, glucose, uric acid (UA), and asc[illegible]ic acid (AA) [illegible]ere purchased from Sigma-Aldrich (USA). Al[illegible]e ch[illegible]micals we[illegible] of analytical reagent grades and used as [illegible]ived [illegible]thout further purification. All the aqueous solutions [illegible] prepar[illegible] in Milli-Q water (18 MΩ cm^{-1}).

2.2. Synthesis, charac[illegible]ation and functionalization of multiwall carbon nanotubes (MWC[illegible])

MWCNTs used in these experiments were prepared by catalytic chemical vapor decomposition (cCVD) method. The experimental conditions and setup used for their preparation have been described previously [33]. In brief, a two zone furnace with a silica tube having provision for flushing gases (Ar and H_2) through benzene vapor was used. The substrate and precursor (100 mg ferrocene and 100 mg naphthalene) were placed in two quartz boats in the cold zone of furnace and the product was collected from the hot zone. The black product so obtained, was purified by sonication in concentrated HCl (ca. 11.6 M) followed by annealing in air at 400 °C. For the COOH functionalization (f-MWCNT), purified MWCNTs were refluxed in concentrated HNO_3 (ca. 15.8 M) for 6 h. The products were characterized by Raman, FTIR spectroscopy, powder X-ray diffraction analysis (XRD) and scanning electron microscopy (SEM).

2.3. Synthesis of Ag/Ag_2O-f-MWCNTs by electrophoretic method

Electrophoretic deposition of silver nanoparticles on multiwall carbon nanotubes [Ag-f-MWCNTs] has been reported previously [34]. In the present work; anodic dissolution of silver electrode was carried out in an aqueous dispersion of functionalized and oxidatively scissioned MWCNTs in order to deposit thin layer of silver on MWCNTs. For this purpose, home-made setup of rotating disk electrode was used (refer Fig. S1 supporting information). The silver disk electrode (2.0 cm diameter) was fixed to a PTFE holder attached to a motor rotating at fixed angular velocity. This assembly was placed vertically in a borosilicate jacket cell containing a stationary silver disk electrode of an identical size fixed horizontally at the bottom of the cell. The two electrodes were placed 1.0 cm apart in a parallel con[illegible]tion. Prior to electrolysis, the silver disks were polished [illegible] 0.2 [illegible] alumina powder and rinsed with copious amount [illegible] Milli-Q wa[illegible] Typically, 10 mg of COOH functionalized MWCNTs [illegible] sonicat[illegible] in 70 mL of Milli-Q water for 1 h and trans[illegible]red in t[illegible]cell[illegible]5 V DC voltage was applied (variable po[illegible] supp[illegible] Apla[illegible]ndia) between the two electrodes immerse[illegible] the [illegible]spersion. The resulting current was initially very sp[illegible] wh[illegible]increas[illegible] monotonously and stabilized at ca. 20 mA[illegible]er 50 min[illegible] [illegible]ver supply was switched-off and the produ[illegible]sited on [illegible] rotating cathode was collected carefully, washed[illegible]h Milli-Q water and vacuum dried. The final prod[illegible]as charac[illegible]ed by UV–vis (Agilent 8453) and Raman sp[illegible]roscopy (Horiba Jobin Yvon, France, λ=632.81 nm, Laser p[illegible]er 1.7 m[illegible] 100× objective lens, 0.9 NA), powder X-ray d[illegible]action an[illegible]sis (XRD) (Bruker D8 with Cu K_α) and scanning elec[illegible] mic[illegible]copy (SEM) (JEOL JSM-6360).

2.4. Preparation of Ag/Ag_2O-f-MWCNTs modified electrodes

The GC electrode with 3.0 mm diameter was polished with 0.05 μm alumina powder and rinsed with Milli-Q water. Fresh dispersion of Ag/Ag_2O-f-MWCNTs was prepared for each experiment by dispersing 2.0 mg of Ag/Ag_2O-f-MWCNTs in 1.0 mL of Milli-Q water with a brief sonication. From this, 5 μL was drop-casted on the pre-cleaned GC disk electrode and dried under vacuum at room temperature. The procedure of drop-casting was repeated twice so that, net 20 μg of sample would spread on 0.070 cm^2 GC electrode. The Ag/Ag_2O-f-MWCNTs modified electrodes were used for the electrochemical measurements.

2.5. Electrochemical measurements

All the electrochemical investigations were performed using Metrohm-Pgstat100 potentiostat/galvanostat with a three-electrode system. Pt wire loop and Hg/HgO/sat. Ca $(OH)_2$ were used as counter and reference electrodes respectively. Ag/Ag_2O-f-MWCNTs modified electrode or home-made 2.0 mm Ag disk electrode (refer supporting information, 1.2) was used as a working electrode. All the measurements were carried out in an air-tight borosilicate glass cell having a provision to fix the electrodes through B-14 standard ground glass joints. Normal atmosphere was maintained during the measurements.

3. Result and discussion

3.1. Characterization of Ag/Ag_2O-f-MWCNTs

The detailed mechanism of electrophoretic dissolution of Ag anode and subsequent coating of silver nanoparticles on

f-MWCNTs to form Ag-f-MWCNTs composite has been described earlier [34]. In the current work, the cathode was rotated at 1400 RPM while carrying out the electrolysis instead of magnetic stirring of the solution to obtain reproducible hydrodynamic control. Fig. 1(a) and (b) shows the typical SEM images recorded on MWCNTs before and after electrophoretic deposition of silver respectively. A comparison of the SEM images indicates differences which can be attributed to the deposition of thin layer of silver on f-MWCNTs (HCOO-MWCNTs, refer Fig. S2 supporting information) subjected to electrophoresis. UV–vis spectra were recorded for f-MWCNTs and Ag/Ag_2O-f-MWCNTs dispersed in water. Absorption maximum at 435 ± 10 nm is attributed to surface plasma resonance peak for the silver. The shoulder at 265 nm is associated with MWCNTs (refer Fig. S3 supporting information). The elemental composition of the Ag/Ag_2O-f-MWCNTs as obtained from EDAX analysis (refer Fig. S4 supporting information) reveals the presence of 90% silver, 1.5% carbon and 7.4% oxygen in atomic percentages, suggesting that a part of the silver is present in the form of silver oxide. The presence of silver oxide in Ag/Ag_2O-f-MWCNT sample can be attributed to the anodic oxidation of silver electrode during electrolysis.

Fig. 2(a) depicts the XRDs of MWCNTs and Ag/Ag_2O-f-MWCNTs samples. The XRD of MWCNTs sample shows a single sharp prominent peak at 26.0° corresponding to the characteristic 002 plane of graphite, while Ag/Ag_2O-f-MWCNTs exhibit peaks at 38.1°, 44.2°, 64.3°, and 77.3° that can be indexed to 111, 200, 220 and 311 crystallographic planes, reported for silver (JCPDS 02-1098) together with small peaks at 27.0° and 32.5° suggesting the presence of MWCNTs and Ag_2O (111) plane (JCPDS 761393) respectively. High X-ray scattering cross section of Ag masks the peaks of graphitic planes in Ag/Ag_2O-f-MWCNTs. Similarly, th presence of Ag_2O is not observed prominently in the XRD due t the reflections from the same being weak and partially merged with the major peaks of Ag. Typical Raman spectra rec d for MWCNTs and Ag/Ag_2O-f-MWCNTs, are shown in Fig. 2(b). Characteristic D, G and 2D bands are observed at around 1300 cm^{-1}, 1570 cm^{-1} and 2650 cm^{-1}, respectively, in both the samples. The small peak at 1130 cm^{-1} in Ag/Ag_2O-f-MWCNTs represents the surface enhanced Raman scattering reported for C–H bend [35,36]. Additionally, Fig. 2b inset shows the peak at 1068 cm^{-1} attributable to the presence of Ag_2O [37]. These results confirm the presence of MWCNT backbone in the rod shape morphology of silver, noted in SEM (Fig. 1b).

3.2. Electrochemical measurements

3.2.1. Cyclic voltammetry

Electrochemical behavior of silver electrode in alkaline solution is governed by three distinct redox s viz. Ag/AgOH/OH^-, Ag/Ag_2O/OH^- and Ag_2O/AgO/OH^- e first couples represent the formation of Ag_2O while the one repr nts the formation of [Ag (I) Ag (III)] oxide [38], hich tively equivalent to AgO phase. Fig. 3(a) and (b) s ws the C re ed on Ag/Ag_2O-f-MWCNTs and Ag dis lectro resp ely, under identical conditions. Three ano peaks (marked as A_1', A_1 and A_2) are observed in both the cases e peaks A_1' and A_1 could be assigned to Ag/AgOH/OH and Ag/Ag O respectively, leading to the formation of Ag_2O phase. The p k A_2 is attributable to the redox couple, Ag_2O/AgO/O facilitating the formation of AgO phase (please Fig. S5 sup ting information). Kinetics of oxidative conv sion of Ag_2O to AgO at A_2 is reported to be a self-auto talytic el rochemical reaction with respect to AgO [38] and elieved be formed via two parallel routes which might yield t type AgO layers. The inner surface layer is plausibly formed th gh electrochemical oxidation together with crystallo ic phase transformation. The outer surface layer "the layer t ards the electrolyte" is probably formed through the electrochemical oxidation of Ag_2O by the hydroxide ions. A plot of peak

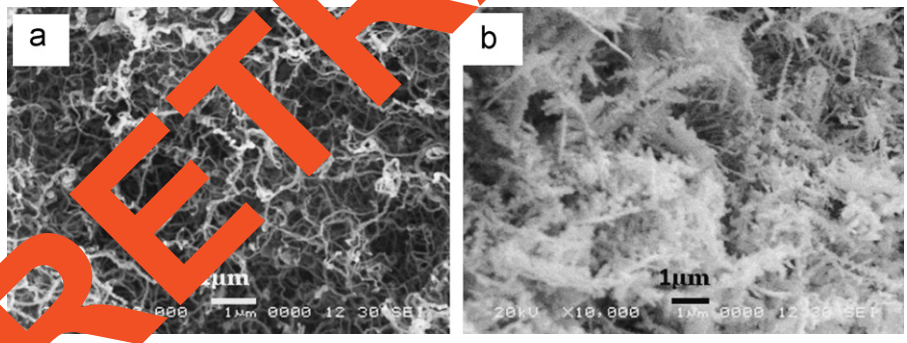

Fig. 1. Typical SEMs of (a) MWCNTs and (b) Ag/Ag_2O-f-MWCNTs.

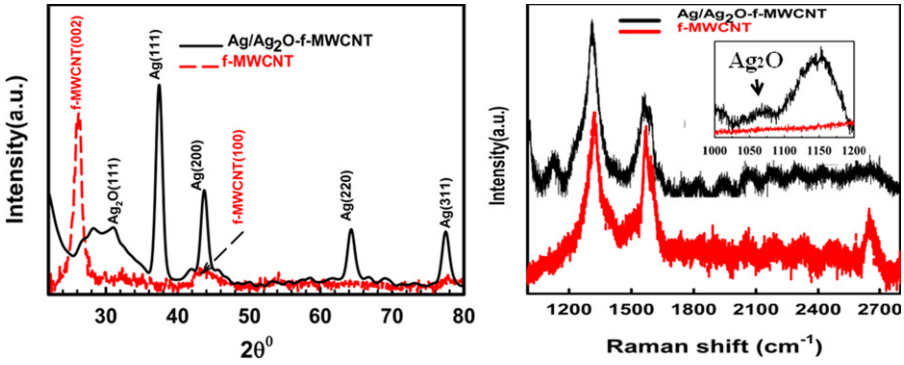

Fig. 2. XRDs and Raman spectra for MWCNTs and Ag/Ag_2O-f-MWCNTs are shown as (a) and (b) respectively. 2(b) inset shows the peak at 1068 cm^{-1} assigned for Ag_2O.

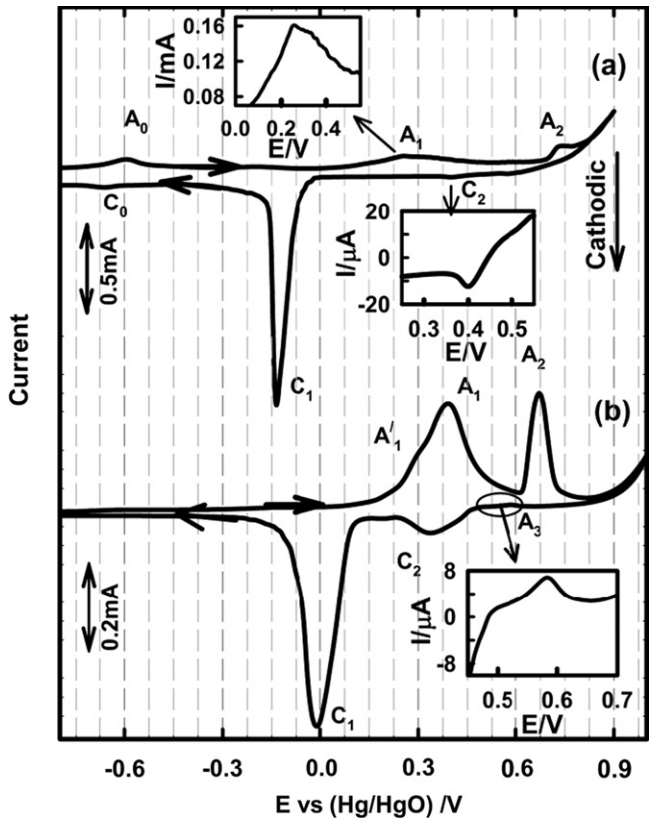

Fig. 3. Cyclic voltammograms of (a) Ag/Ag_2O-f-MWCNTs modified electrode (b) Ag disk electrode recorded in 0.1 M NaOH at scan rate of 100 mVs^{-1}. The insets are enlarged portions of the CVs indicated by the arrows.

current at A_2 vs. square-root of scan-rate for Ag/Ag_2O-f-MWCNTs electrode fitted in a straight line with $R^2=0.9$ (refer Fig. S6 supporting information) suggests the process is diffusion controlled electron transfer reaction. However, in case of Ag disk electrode, the peak position does not show any shift above the scan rate of 200 mVs^{-1} (plot is not shown), indicating that the formation of AgO is rather charge transfer controlled.

After scan reversal, the silver disk electrode shows a weak anodic peak (marked as A_3) associated with completion of AgO formation. The nuclei of AgO are formed at Ag_2O surface during the forward scan thus further formation of AgO becomes easier than initial formation and autocatalytic formation of AgO is completed at low potential [38] (refer Fig. 3(b) and its inset). The first peak at 0.58 V is attributed to the oxidation of Ag_2O (outer surface layer) to AgO and second one just before peak C_2 is due to oxidation of Ag_2O to AgO at inner surface layer [31]. These peaks are not legible in case of Ag/Ag_2O-f-MWCNTs, as the oxidation of thin layer of silver present on the surface of f-MWCNT gets completed during forward scan and there is less possibility of presence of predominant Ag_2O at inner surface layer. This electrochemical behavior of Ag/Ag_2O-f-MWCNTs electrode is advantageous, thus enabling the measurement of current produced due to electrochemical oxidation of glucose. On proceeding towards lower potential, AgO is reduced to Ag_2O (cathodic peak marked as C_2 (refer Fig. 3(a) lower inset) and subsequently to Ag (0) (marked as C_1). Furthermore, a weak quasi-reversible couple (marked as A_0 and C_0) observed at −0.6 V during cathodic scan can be attributed to the adsorption/desorption of hydroxyl groups on the silver surface [39], more prominent in case of Ag/Ag_2O-f-MWCNTs electrode due to the high surface area.

In case of Ag/Ag_2O-f-MWCNTs electrode, C_1 is found to be substantially large compared to the disk electrode. The ratio of coulombs under the cathodic and anodic peaks in closed potential cycles were compared in both the cases. For Ag/Ag_2O-f-MWCNTs, the ratio is ~2.30. The ratio is expected to be 1.00 when the charges in the redox reactions are balanced which is indeed observed in case of disk electrode with the value being 0.98. The charge imbalance shown by Ag/Ag_2O-f-MWCNTs is probably due to the anomalously high contribution from C_1 towards the reduction of Ag_2O to Ag. These results confirm the presence of native Ag_2O on the surface of f-MWCNTs prior to the electrochemical oxidation. These observations are concomitant with the EDAX analysis of Ag/Ag_2O-f-MWCNTs sample.

In case of Ag/Ag_2O-f-MWCNTs, A_1 appears at less positive potential (−0.14 V), while A_2 shifts towards higher potential (+0.05 V). On the other hand, C_1 is seen to shift towards more negative potential (−0.12 V) compared to the disk electrode. These observations suggest that Ag_2O present in Ag/Ag_2O-f-MWCNTs is relatively more reversible, its formation being easier (negative shift in A_1), whereas the reduction is difficult indicated by the negative shift in C_1. This superiority of the composite is attributable to the electrocatalytic activity characteristic of MWCNTs which stabilize the AgO phase associated with Ag/Ag_2O-f-MWCNTs.

Fig. 4(a) and (b) depicts the electrochemical behavior of Ag/Ag_2O-f-MWCNTs and Ag disk electrodes, respectively, recorded in the presence of 5 mM glucose in 0.1 M NaOH. For comparison, the CVs recorded in the absence of glucose (refer Fig. 3), are superimposed as dotted curves. On addition of glucose, the CV obtained for Ag/Ag_2O-f-MWCNTs shows increase in the intensities of the anodic peaks (A'_1, A_1 and A_2) and a sharp decrease in the cathodic C_2 peak. Increase in the peak heights of A_1 and A_2 indicates an increase in the rate of conversion of Ag→Ag_2O, in the presence of glucose due to increase in the reactant

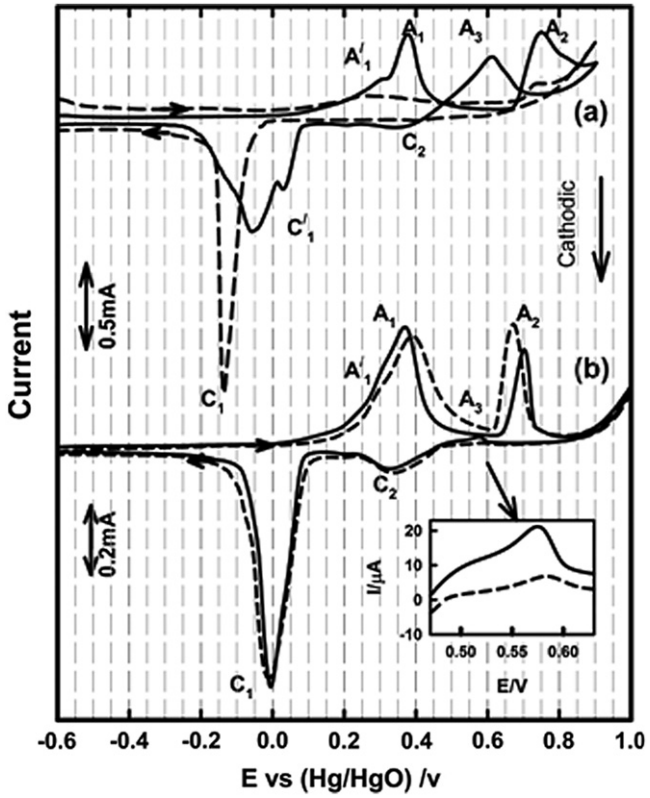

Fig. 4. Cyclic voltammograms of (a) Ag/Ag_2O-f-MWCNTs modified electrode (b) Ag disk electrode recorded in 0.1 M NaOH and 5 mM of glucose at a scan rate of 100 mVs^{-1}. CVs recorded without glucose (refer Fig. 3) are superimposed as dotted curves. The insets are enlarged portions of CVs indicated by the arrows.

concentrations i.e. [Ag] and [OH^-]. Since [OH^-] was in excess and thus remained constant, the increase in rate is because of increase in the concentration of Ag (0) available for the reaction. This is possible only when the native Ag_2O on Ag/Ag_2O-f-MWCNTs surface reacts with glucose and reduces to Ag (0). On the contrary, decrease in the peak height at C_1 suggests decrease in the surface concentration of Ag_2O as a result of chemical reaction with glucose. In order to support this, the CVs were recorded by holding the potential at +0.2 V (just before A_1) for various time intervals (please refer Fig. S7 supporting information). This potential was selected as Ag_2O does not form at this potential (refer Fig. 4). Apart from this, a new large anodic peak (A_3) appears at ~+0.6 V in the reverse scan representing the electrochemical re-oxidation of Ag_2O formed due to glucose oxidation (A_2) on the electrode surface to AgO (indirectly representing the amount of glucose in the solution). Besides these features, Ag/Ag_2O-f-MWCNTs show a prominent shoulder marked as C_1^l which is found to be complimentary with A_1^l and attributed to the reduction of AgOH back to silver. In case of Ag disk electrode, the intensity of peak A_1 is similar as in the absence of glucose since there is no native silver oxide present on the surface of electrode compared to Ag/Ag_2O-f-MWCNTs electrode while that of A_2 peak shows a negligible decrease [30] since the outer surface layer of AgO available on the electrode for glucose oxidation is less and the inner layer transformation of Ag_2O to AgO is perhaps not much affected in the presence of glucose due to geometrical hindrance of the surface layer. Further, Ag_2O formed through glucose oxidation (A_2) would get re-oxidized to AgO at A_3 so the current at peak attributed to outer surface of oxide layer show increase in A_3 (refer Fig. 4b). No appreciable current changes were observed on the C_1 peak for the disk electrode (refer Fig. 4b).

Based on the CV measurements, the steps involved in th glucose oxidation on Ag/Ag_2O-f-MWCNTs are summarized a follows

Forward Scan:

(a) $nAg/Ag_2O + Glucose \xrightarrow{2H^+,2e^-} (n+2)Ag + H_2O + gluc$ ctone (A_1)

(b) $nAg + 2OH^- \rightarrow (n-2)Ag/Ag_2O + H_2O + 2e^-$ (A_1)

(c) $Ag/nAg_2O + 2OH^- \rightarrow Ag/(n-1)Ag_2O/2$ r-layer) + O + $2e^-$ (A_2)

(d) $nAg/Ag_2O \rightarrow (n+1)Ag/AgO(In$ -layer e^- (A_2)

(c′) $Ag/nAgO + Glucose \xrightarrow{2H^+,2e^-} Ag/(n$ AgO/ O + glucolactone (A_2)

Reverse Scan:

(f) $Ag/nAgO/Ag_2O + 2O$ $Ag/(n+2)AgO + H_2O + 2e^-$ (A_3)

(g) $Ag/2AgO + H_2O + 2e^- \rightarrow Ag$ $g_2O + 2OH^-$ (C_2)

(h) $nAg/Ag_2O + H_2O + e^- \rightarrow (n+2)Ag + 2OH^-$ (C_1)

Further, the potential applicability of this system as a glucose sensor was investigated by recording the CVs of Ag/Ag_2O-f-MWCNTs electrode at various glucose concentrations (2–10 mM) keeping all other parameters constant, Fig. 5. As expected, the intensity of peak A_2 was observed to decrease while that of peak A_3 increased indicating a correlation between glucose concentration and the peak current at A_3 (step *f*). The decrease in the intensity of peak at A_2 is because of higher degree of conversion of AgO to Ag_2O with glucose concentration. However, the Ag_2O formed would convert back to AgO exhibiting peak A_3 at ~0.6 V, increasing proportionately with glucose concentration (step *f*). A plot of A_3 peak current vs. glucose concentration shows a linear nature (refer Fig. 5 inset) with $R^2 = 0.992$ thus supporting

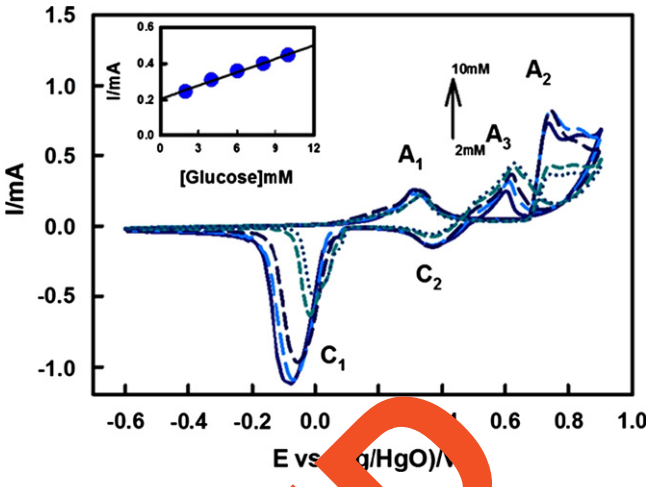

Fig. 5. Cyclic voltammograms re ed for Ag_2O-f- CNTs modified electrode in 0.1 NaOH and varying ose concent 10 mM) at scan rate of 50 mV s^{-1}. The inset shows a t of pe current vs. glucose concentration. The filled circles are experi al p and solid line corresponds to the fitting in the linear regression

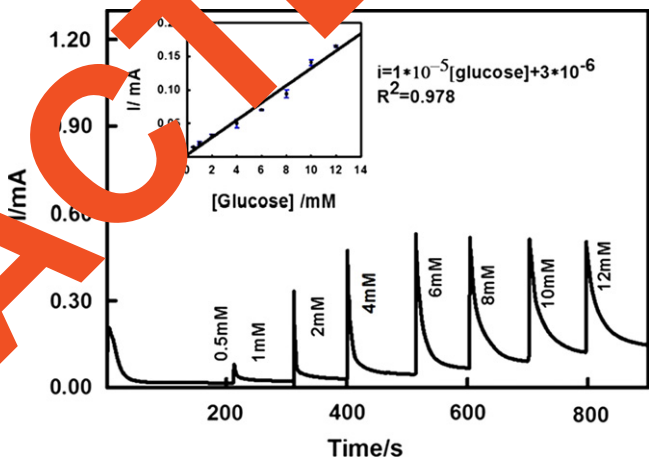

Fig. 6. Current–time dynamic response of Ag/Ag_2O-f-MWCNTs electrode at step potential of 0.6 V in 0.1 M NaOH and varying glucose concentrations (0.5–12 mM) added at intervals of 100 s. Inset shows the plot of limiting current vs. the glucose concentration. Standard deviation bars were generated for 10 repetitions.

the monitoring of glucose on Ag/Ag_2O-f-MWCNTs modified electrode.

The difference in the number of coulombs between the cathodic and anodic peaks observed in CVs recorded at various concentrations of glucose was also fitted in the linear regression plot with $R^2 = 0.999$ (refer Fig. S8 and Table. S1, in the supporting information). This observation suggests the complete balancing of charges and concentration of glucose and there is no apparent side reaction involved in the potential cycle other than the glucose oxidation.

3.2.2. Amperometric detection of glucose

Fig. 6 shows the amperometric response of Ag/Ag_2O-f-MWCNTs electrode to successive addition of glucose concentrations (0.5–12 mM) in 0.1 M NaOH and applied potential of +0.6 V. The choice of applied potential is based on the results of cyclic voltammetry which shows the absence of anodic peak at A_3 in the absence of glucose at the same electrode (Ag/Ag_2O-f-MWCNTs), thereby, allowing the measurement of current at A_3 peak due to re-oxidation of Ag_2O (formed at A_2) to AgO upon

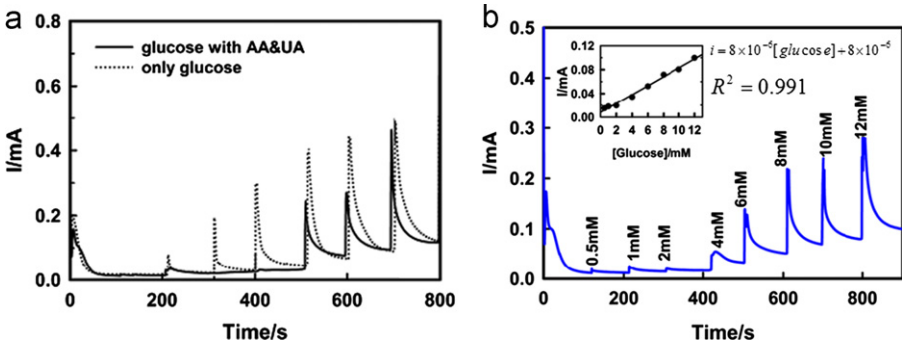

Fig. 7. (a) Current–time dynamic response of Ag/Ag_2O-f-MWCNTs modified electrode at the step potential of 0.6 V with stepwise addition of glucose (0.5–12 Mm) in 0.1 M NaOH together with 0.1 mM of ascorbic acid, and 0.02 mM of uric acid. The limiting currents were sampled after every addition. (b) Current–time dynamic response of Ag/Ag_2O-f-MWCNTs electrode at step potential of 0.6 V in 0.1 M NaOH, 0.2 M NaCl and varying glucose concentrations (0.5–12 [illegible] at intervals of 100 s. Inset shows the plot of limiting current vs. the glucose concentration.

addition of glucose as mentioned earlier (Fig. 4a). Also, the highest sensitivity for working electrode obtained at the same potential. The sensor shows linear range between 0.5 and 12 mM glucose concentration, the best linear fit is plotted with a linear regression of 0.978, the limit of detection and the sensitivity are worked out to be 5.5 μM(S/N=3) and 17 μA mM^{-1} cm^{-2} respectively (for details cf. supporting information 2.1 and 2.2). To our knowledge, this is for the first time that these values are being reported for Ag/Ag_2O-f-MWCNTs in the amperometric detection of glucose.

3.3. Interference studies on Ag/Ag_2O-f-MWCNTs modified electrode

During glucose detection, interference in the measurement [illegible] usually caused by readily oxidizable species such as ascorbic ac[illegible] (AA) and uric acid (UA), present in the blood ser[illegible] Though present in small concentrations AA and UA (c[illegible] 0.1 [illegible] and 0.02 mM, respectively), interfere in the meas[illegible]ments due to high rate constants for their oxidation [40]. Fig. [illegible] current–time profile recorded in a set of e[illegible]eriment[illegible] carried out with increasing concentration of gluco[illegible]ping that [illegible]A and AA constant. The response is similar [illegible] bo[illegible]e cases (presence and absence of UA and AA) in the [illegible]wer concen[illegible]ion range from 0.5 to 4 mM while a negligibl[illegible]ifference is obs[illegible]ed at higher concentrations. Cl^- is an[illegible]r co[illegible]ituent in the biological samples which is known to p[illegible] [illegible]etal [41] and alloy [8] based glucose sensors. Fig. 7(b) sho[illegible] the [illegible]rrent–time dynamic response recorded [illegible] gl[illegible]se in [illegible]resence of 0.2 M NaCl. The limiting curre[illegible] was s[illegible]pled afte[illegible] every addition of glucose and the calibration [illegible]v[illegible]sor is shown as inset of figure. From the slope, [illegible]itivity calculated was obtained as 17 μA mM^{-1} cm^{-2}, wh[illegible] is identical to that noted in the absence of chloride ions (refer Fig. 7(b) Inset). This set of experiments indicated that the presence of chloride ions has no effect on the practical performance of Ag/Ag_2O-f-MWCNTs towards the detection of glucose.

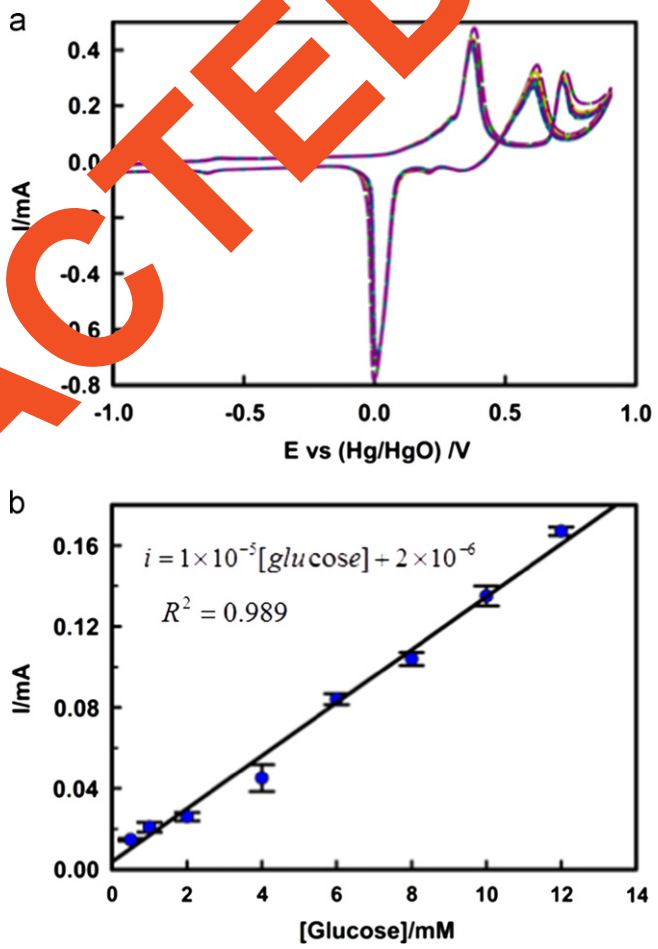

Fig. 8. (a) Cyclic voltammograms recorded for Ag/Ag_2O-f-MWCNTs modified electrode in 0.1 M NaOH and 5 mM glucose solution at a scan rate of 100 mVs^{-1}(25 cycles). (b) Calibration curve of studied electrode with error bars obtained from five calibrations for five different electrodes constructed identically.

3.4. Stability and reproducibility of Ag/Ag_2O-f-MWCNTs modified electrode

Stability of Ag/Ag_2O-f-MWCNTs modified electrode for the glucose oxidation was examined by performing repeated cycle CV measurements in the potential range −1.0 to +0.9 V (Fig. 8a). Neither apparent change in the CV profile nor shift in the peak potentials with the repetition of scans was observed. From these observations, no apparent degradation of the Ag/Ag_2O-f-MWCNTs surface was inferred. Marginal decrease in the current values (~10%) for all the peaks is attributed to the decrease in the glucose concentration near the surface due to continuous cycling. The reproducibility of sensor was evaluated by performing experiments on five electrodes modified identically with Ag/Ag_2O-f-MWCNTs and current responses were recorded after subsequent addition of glucose at +0.6 V for each one of them. Fig. 8b, illustrates the calibration curve for the studied electrodes with error bar obtained from five calibrations of five different identical electrodes. The relative standard deviation (RSD)

calculated for each addition is given in Table S2. The RSD (1.2–5.3%) values confirm the reproducibility of results (Table S2).

4. Conclusion

Herein, we demonstrate the use of novel Ag/Ag_2O-f-MWCNTs composite for the non-enzymatic detection of glucose. Ag/Ag_2O-f-MWCNTs composite electrode shows different catalytic behavior compared to silver disk electrode. The MWCNTs backbone contributes towards stability and performance of Ag/Ag_2O-f-MWCNTs in the glucose detection. MWCNTs also render mechanical support which seems to be very important when Ag is repeatedly phase transformed from $Ag \leftrightarrow Ag_2O \leftrightarrow AgO$ during glucose oxidation. Based on the shift in the peak potentials in the CV measurements, Ag_2O phase is found to be stable in Ag/Ag_2O-f-MWCNTs; these features are attributed to the electron withdrawing properties of MWCNTs. Large surface to volume ratio of the composites is found to be advantageous for a strong electrochemical response due to glucose oxidation reaction. The Ag/Ag_2O-f-MWCNTs modified electrode exhibits good electrocatalytic ability for glucose oxidation in alkaline solution, high sensitivity even in the presence of Cl^-, negligible interference from UA and AA and good stability and reproducibility in the concentration range between 0.5 and 12 mM. Therefore, it can be used as an electrochemical (amperometric) sensor for detection of glucose in clinical applications.

Acknowledgment

The financial support from the DBT, government of India [illegible] acknowledged. The authors appreciate Department of Physics, University of Pune for SEM and XRD facilities; they also acknowledge Prof. Pavankumar, ISER, Pune for Raman spectr[illegible]Prof. Nanda Haram for the fruitful discussion.

Appendix A. Supporting information

Supplementary data associated with this artic[illegible]an be found in the online version at http://dx.doi.org/[illegible]1016/j.tala[illegible]2012.11.019.

References

[1] S. Wild, G. Roglic, A. Green, R. Sicree, H. King, Diabetes Care 27 (2004) 1047.
[2] E.M. Benjamin, Clin. Diabetes 20 (2002) 45.
[3] J. Wang, Chem. Rev. 108 (2008) 814.
[4] S. Park, H. Boo, T.D. Chung, Anal. Chem. Acta 556 (2006) 46.
[5] S. Cho, H. Shin, C. Kang, Electrochim. Acta 51 (2006) 3781.
[6] E. Skou, Electrochim. Acta 22 (1997) 313.
[7] J.M. Marioli, T. Kuwana, Electrochim. Acta 37 (1992) 1187.
[8] Y. Sun, H. Buck, T.E. Mallouk, Anal. Chem. 73 (2001) 1599.
[9] S.B. Hocevar, B. Ogorevc, K. Schachl, Kurt Kalcher, Electroanalysis 16 (2004) 1711.
[10] G.L. Luque, M.C. Rodnguez, G.A. Rivas, Talanta 66 (2005) 467.
[11] S. Ernest, J. Heitbaum, C. Hamann, Electroanal. Chem. 100 (1979) 173.
[12] C. Su, C. Zhang, G. Lu, C. Ma, Electroanalysis 22 (2010) 1901.
[13] X. Ren, X. Meng, F. Tang, Sensors Actuators B 110 (2005) 358.
[14] X. Chen, H. Pan, H. Liu, M. Du, Electrochim. Acta 56 (2010) 636.
[15] H. Quan, S.U. Park, J. Park, Electrochim. Acta 55 (2010) 2232.
[16] F. Sun, L. Li, P. Liu, Y. Lian, Electroanalysis [illegible]011) 395.
[17] A. Gutes, C. Carrari, R. Maboudian., Ele[illegible]a 56 (2011) 5855.
[18] J. Li, R. Yuan, Y. Chai, X. Che, W. Li, X. [illegible]ng, Micro[illegible]. Acta 172 (2011) 163.
[19] Z. Zhuang, X. Su, H. Yuan, Q. Sun, [illegible]o, Analyst [illegible](2008) 126.
[20] Md.M. Rahman, A.J.S. Ahmmad, J.H. J[illegible]L. Ahn, J.J[illegible]e, Sensors 10 (2010) 4855.
[21] P.C. Biswas, Y. Nodasaka, M[illegible]yo, M. Haru[illegible]oanal. chem. 381 (1995) 167.
[22] F. Kurinawan, V.M. Mi[illegible] Ele[illegible]talysis 18 (2006) 1937.
[23] J.S. Ye, Y. Wen, W[illegible] Zha[illegible]. Gan, C[illegible]Xu, F.S. Sheu, Electrochemistry Comm. 6 (2004[illegible].
[24] H. Zhu, X. Lu[illegible] Y. Shao, Z.[illegible]anta 79 (2009) 1446.
[25] Y. Myung[illegible] Y.J. Cho, H.S[illegible]m, J. Park, J.U. Kim, Y. Choi, C.J. Lee, J. Phys. Chem. C 113 [illegible]9) 1251.
[26] J. Yan[illegible] C. Jiang, W.B[illegible]ng, S. Gunasekaran, Talanta (2010) 25.
[27] X[illegible], Z.J. Lin, D.J. C[illegible]T.T. Jia, Z.M. Cai, X.R. Wang, X. Chen, G.N. Chen, [illegible]yama, Biosens. Bioelectron. 25 (2010) 1803.
[28] [illegible]. Rong, C. Y[illegible], Q.Y. Qian, X.H. Xia, Talanta (2007) 819.
[29] [illegible]un, J. Zhen[illegible]. Sheng, Electrochim. Acta 65 (2012) 64.
[30] T[illegible]ougas, M[illegible]ebenedetto, J.M. DeMott Jr., Electroanalysis 5 (1993) 669.
[31] J.M[illegible]L.D.G.E. Jahngen, Electroanalysis 17 (2005) 599.
[32] H.Ng. K[illegible], H. Liu, R.M. Penner, Langmuir 16 (2000) 4016.
[33] [illegible]M. Samant, S.K. Haram, S. Kapoor, Pramana J. Phys. 68 (2007) 51.
[34] [illegible]mant, V.R. Chaudhari, S. Kapoor, S.K. Haram, Carbon 45 (2007) 2126.
[35] Y.C. Tsai, P.C. Hsu, Y.W. Lin, T.M. Wu, Electrochem. Comm. 11 (2009) 542–545.
[36] Y.C. Tsai, P.C. Hsu, Y.W. Lin, T.M. Wu, Sensors Actuators B 138 (2009) 5.
[37] G.R.I.N. Waterhouse, G.A. Bowmaker, J.B. Metson, Phys. Chem. Chem. Phys. 3 (2001) 3838.
[38] P. Stonehart, F.P. Portante, Electrochim. Acta 13 (1968) 1805.
[39] E.R. Saviniva, A. Scheybal, M. Danckwerts, U. Wild, B. Pettinger, K. Doblhofer, R. Schlogl, G. Erel, Faraday Discuss. 121 (2002) 18.
[40] S. Park, T.D. Chung, H.C. Kim, Anal. Chem. 75 (2003) 3046.
[41] Y.B. Vassilyev, O.A. Khazova, N.N. Nikolaeva, J. Electroanal. Chem. 196 (1985) 105.